Asian Journal of Chemistry; Vol. 37, No. 11 (2025), 2855-2864
ASIAN JOURNAL OF CHEMISTRY
https://doi.org/10.14233/ajchem.2025.34658

Development of Novel Caffeine-Loaded Polyvinyl Alcohol Nanofabric Face Wipe: A Comparative Electrochemical Release Profiling using Bare and Modified Electrodes

K.V. SAYANA, MANOJ HEBRI and T. VISHWANATH*,

Department of Materials Science, Mangalore University, Mangalore-574199, India

*Corresponding author: E-mail: vishutcg@gmail.com

Received: 7 August 2025 *Accepted*: 9 October 2025 *Published online*: 27 October 2025 AJC-22176

This study presents the preparation and electrochemical evaluation of a novel caffeine-infused nanofabric designed for controlled topical delivery. The caffeine-infused PVA nanofabric was prepared using electrospinning technique and characterized by spectral and analytical methods. The nanofabric was formulated to gradually release caffeine upon wetting and the release profile was monitored at different time intervals. Quantification of the released caffeine was carried out using linear sweep voltammetry (LSV), employing both a bare glassy carbon electrode (GCE) and a modified GCE (MGCE) fabricated by electrospinning a nanocomposite of polyvinyl alcohol (PVA), Multiwalled carbon nanotubes (MWCNT) and graphene oxide (GO). Calibration curves using standard caffeine solutions demonstrated excellent linearity for both electrodes, with enhanced sensitivity, especially observed in MGCE (R^2 = 0.999) compared to the GCE (R^2 = 0.997). The modified electrode also exhibited lower limits of detection (LOD = 0.042 mg/mL) and quantification (LOQ = 0.139 mg/mL), confirming its superior analytical performance. Cyclic voltammetry (CV) at varying scan rates revealed a purely diffusion-controlled process for GCE, while the modified electrode indicated a mixed diffusion-adsorption mechanism. The maximum release of caffeine from the wipe was achieved at 30 min, establishing its efficiency as a sustained-release skincare application. This work also highlights the potential of combining electrospun nanofiber-modified electrodes with electrochemical techniques for evaluating the performance of face wipe fabric.

Keywords: Caffeine, Electrospinning, Electrochemical sensor, Polyvinyl alcohol, Face wipe.

INTRODUCTION

Among the diverse branches of the global textile industry, medical textiles are emerging as a rapidly expanding and highly dynamic sector [1]. Products like surgical coverings, drapes, clothing, blankets, sheets, incontinence diapers, wipes and other items fall within the significant category of medical textiles known as healthcare and hygiene products [2]. Wipes, categorized under medical textiles, are single-use cloths infused with cleaning agents and commonly used for personal hygiene. Wipes are widely used for facials, infant care and other personal hygiene purposes due to their comfort and ease of use. They are commonly manufactured from fibers such as polyester, polyethylene, cotton, viscose, *etc*. and are available commercially in both disposable and flushable forms [3,4]. Wipes are categorized as two types, namely wet and dry wipes, are disposable cleansing products, their moisture content and usual applications vary. While wet wipes are pre-moistened with cleaning agents, alcohol, fragrance, *etc*. [5]. Dry wipes offer flexible use, whether dry or dampened with water or cleaning agents [6]. Prepared from cotton, paper or non-woven fabrics, they are commonly employed for cleaning, dusting, and medical purposes. However, a significant drawback is that the synthetic fibres are not biodegradable and cause contamination from microplastics. Furthermore, the finishing chemicals may be rough on the skin, resulting in inflammation, allergies, *etc*. [7].

Like any other industry, the cosmetics sector is highly diversified in order to meet customer needs for well-maintained personal care goods and to enhance quality. Nanomaterials have been used into a greater range of cosmetic goods [8], including sunscreen creams [9], anti-aging creams [10], hair products [11], facial masks [12] and lipsticks [13]. A lot of focus has been placed on creating face masks or membranes that can release skincare products in the burgeoning field of electrospun nanofiber cosmetics [14,15]. Using synthetic polymers like polyvinyl alcohol [16], polyvinyl pyrolidone (PVP) [17] and polyethylene oxide [18] as well as polymer solutions

like cellulose acetate [19], chitosan [20] and hyaluronic acid [21], electrospinning is an inexpensive and adaptable method [22] for creating nanofibers for various cosmetic applications. The ability to use any active chemicals of interest when creating the fibrous mat is the primary benefit of the electrospinning approach. Moreover, electrospun fiber masks are effective at releasing active chemicals, don't require preservatives and can be packaged as dry sheets [23]. They must only be wetted at the appropriate moment in order to release active chemicals [24]. These have mostly been used to release substances for skin healing [25], therapy and cleansing [26] because of their capacity to facilitate improved contact with the skin, facilitating a deeper penetration of the active agent [27]. Using the electrospinning technique, researchers developed a nanofibrous face wipe incorporating biocompatible PVA infused with matcha green tea extract. PVA, a low-cost synthetic amphiphilic polymer, is widely utilized in various applications including cosmetic formulations due to its hydrophilic nature, biocompatibility, biodegradability and non-toxicity [28,29]. A study reported the use of PVA as a secondary material in the production of wipes, where 2% to 10% by weight of untreated, water-soluble PVA fibers were heat-bonded to a matrix of absorbent fibers. This process resulted in a nonwoven fabric that is absorbent, flushable, biodegradable, and medically safe, with PVA acting as the binding component. The resulting material is well-suited for various applications, including wraps, wipes, absorbent pads, and other healthcare-related products. Low quantities of PVA fibers give softness and provides adequate wet strength [30].

Caffeine is a natural stimulant commonly found in tea, coffee, cola, chocolate and energy drinks. Among the beverages, matcha tea contains relatively high amount of caffeine compared to other teas [31-33]. It belongs to a class of compounds called xanthine and is best known for its stability. Caffeine has several benefits for the skin which is why its common ingredient in skincare products. It is proved that caffeine can reduce the puffiness and dark circles by constricts blood vessels [34]. Also, it soothes the inflammation by act as an anti-inflammatory agent that can reduce irritated skin and acne [35]. It is having antioxidants protect skin from damage caused by free radicals and environmental factors like UV rays and pollution [36]. It is well-known for slow down the aging process by erasing the signs like fine lines and wrinkles [37]. In recent years, caffeine has garnered significant interest in the field of dermatology and skincare, particularly for its potential role in enhancing skin appearance, reducing puffiness and combating signs of aging. As a result, there has been an increasing demand for caffeine-based topical formulations such as creams, gels and face wipes. Caffeine can provide a firmer toned skin appearance by increasing the blood flow and give a temporary clean and glowing skin texture [38]. It helps to regulate the oil production on skin which help people with sensitive acne prone skin. Most of the cosmetic and skin care products like creams, serum and eye-creams contain caffeine as a component functioning as a rejuvenation of skin and eyes [39]. Simultaneously, accurate detection and quantification of caffeine released from such systems are essential for understanding release kinetics and ensuring formulation efficacy. The electrochemical sensing offers a rapid, sensitive and cost-effective method for caffeine detection. Glassy carbon electrodes (GCE) are commonly used in electrochemical sensors due to their wide potential window, low background current and chemical inertness. To improve the sensitivity and signal response of the electrode, surface modification with nanomaterials such as carbon nanotubes (CNT) and graphene oxide (GO) has proven effective due to their high conductivity, surface area and synergistic interactions with analytes [40].

The majority of wipes that are widely used and sold commercially nowadays are composed of synthetic fibres that have been moistened with chemicals. To get beyond this eco-friendly herbal completed wipes are the best option. This article addresses the impacts and application of sustainable face wipe using biodegradable materials and herbal compounds. Some brands are flushable wipes that break down in water, but very few contain biodegradable fibres. Pure herbal extract finished wet wipes are still in the research stage and not yet on the market. For the benefit of present and future consumers, manufacturers and customers alike must be aware of the need for sustainable wipes. In this work, a GCE was used for electrochemical quantification of caffeine released from the PVA-based face wipe and its performance was compared with that of a modified electrode. This integrated approach not only explores the development of a caffeine-loaded electrospun face wipe but also presents a robust and comparative electrochemical analysis using bare and modified electrodes. The study demonstrates the feasibility of using such a sensor platform for evaluating the release profile and detecting low concentrations of caffeine in topical delivery systems.

EXPERIMENTAL

Caffeine (≥ 99% purity), potassium chloride (KCl), polyvinyl alcohol (PVA), carbon nanotubes (CNT) and graphene oxide (GO) were procured from SRL Pvt. Ltd. All aqueous solutions were prepared using double-distilled water. Commercial matcha green tea powder was purchased from the local distributor of Goa state, India.

Preparation of caffeine from tea extract: In a hot 100 mL of deionized water, 10 g of tea powder was added and boiled for 15 min. The mixture was filtered and the extract was cooled to room temperature. Then 2.5 g of Na_2CO_3 was added and stirred until fully dissolved. The solution was further cooled in an ice bath and transferred to a 250 mL separating funnel. It was then extracted with 20 mL of dichloromethane (DCM). After phase separation, the lower organic layer was collected into a clean beaker, ensuring no aqueous or emulsified material was included. The extraction was repeated twice using fresh 20 mL portions of DCM, and all organic layers were combined. The final extract appeared clear and colourless.

Electrospinning of face wipe fabric: Stirred PVA (8 wt.%) in deionized water at 45 ºC for 1 h on a magnetic stirrer followed by the addition of 10 mL of extracted caffeine with PVA solution. The prepared PVA/caffeine solution was then loaded into a 5 mL plastic syringe. A voltage of 15 kV, with a tip-collector distance of 12 cm was applied to the spinning solution and fibers were collected on a drum collector with rotation of 300 rpm for 15 min at 0.9 mL/h flow rate.

Modification of glassy carbon electrode (GCE): The GCE was modified by electrospinning of a nanocomposite

PVA solution. For this, 0.5 mg of MWCNTs and 0.5 mg of GO were dispersed in 2 mL of 7 wt.% PVA solution. The mixture was sonicated to achieve uniform dispersion. Electrospinning was carried out for 10 min at an applied voltage of 15 kV, a flow rate of 0.9 mL/h and a collector rotation speed of 300 rpm and nanofibers were collected on the glassy carbon electrode.

Electrochemical analysis: All electrochemical experiments were performed using a three-electrode system comprising the bare or MGCE as the working electrode, a platinum wire as counter electrode and an Ag/AgCl electrode as reference. The linear sweep voltammetry (LSV) was employed for quantification, while CV was conducted at scan rates ranging from 10 to 200 mV/s to determine the nature of the electrochemical process (diffusion or adsorption controlled). The reaction behaviour was confirmed by plotting peak current (I_p) *vs.* square root of scan rate ($\nu^{1/2}$) and log I_p *vs.* logν.

Characterization: The Fourier transform infrared (FTIR) spectrum of face wipe fabric was recorded on a Shimadzu FT-IR-157 spectrometer. The X-ray diffraction (XRD) patterns were recorded in reflection mode in the angle range (2θ) on a Rigaku Miniflex 600 diffractometer using Cu*K*α source. The electron microscopic images of nanofibers were recorded using a Carl-Zeiss field emission scanning electron microscope (FE-SEM). The differential scanning calorimetric (DSC) and thermogravimetric analysis (TGA) of the face wipe fabric was carried out on the Perkin-Elmer STA600 Thermal analyzer. The tensile properties of the fabric were determined using a Universal testing machine (UTM) ASI-AMT-2BC followed by the ASTM D882 procedure.

Water uptake test: Following a previously described protocol with a small modification [41], the water absorption test and solubility test were carried out. The fabrics were divided into five sections of 10 mm × 30 mm. The desiccator was used to keep the dry samples prior to testing. The amount of water absorbed was determined by placing each dried film in a separate 70 mL of Milli-Q water in a beaker while swirling continuously for 1 h at 25 ºC. Using filter paper, the samples were collected and dried. Once the water had been completely removed from the film surface, it was weighed once again. The following formula was used to obtain the average value of water uptake:

$$\text{Water uptake (\%)} = \frac{W_s - W_d}{W_d} \times 100 \quad (1)$$

where W_s is the weight of swollen sample; and W_d is the weight of dried sample.

Solubility test: For the purpose of measuring solubility, the face wipe fabric was sliced into 10 mm × 30 mm dimensions and dried in a hot air oven. Separately, the dried fabrics were dipped into a beaker containing 70 mL of Milli-Q water and swirled for 1 h at 25 ºC. The excess water of the swelled film was removed with the help of filter paper after the film had been continuously stirred and weight was recorded. The film samples were fully dried in a hot air oven until reached a constant weight. The solubility of each film was calculated using eqn. 2; data was collected in triplicate [42].

$$\text{Solubility (\%)} = \frac{W_i - W_f}{W_i} \times 100 \quad (2)$$

where W_i is the initial dry weight; and W_f is the final dry weight

Electrochemical study

Preparation of standard caffeine solutions: A stock solution of caffeine (10 mg/mL) was prepared by dissolving 1000 mg of pure caffeine in 100 mL of distilled water. From this stock, standard solutions of concentrations 0, 0.5, 1.0, 1.5, 2.0, 3.0 and 5.0 mg/mL were prepared by appropriate dilution. Each of these solutions was mixed with 0.1 M KCl to maintain a constant ionic strength and the total volume was adjusted to 10 mL in each case. The LSV measurements were performed using a GCE to obtain the calibration data.

Release study from caffeine-impregnated face wipe: Caffeine-impregnated face wipes were soaked in 10 mL of distilled water and samples were collected at intervals of 5, 10, 15, 20, 25 and 30 min. Each sample was then mixed with 0.1 M KCl before LSV analysis using both bare and modified GCEs. The peak current data were compared with the calibration curve to quantify the caffeine released at each time point.

RESULTS AND DISCUSSION

Morphological and structural studies: A dense, interconnected fibrous network was observed (Fig. 1a), with noticeable bead-like formations distributed across the fiber surface. These bead structures are typically indicative of rapid solvent evaporation and a reflect localized accumulation of MWCNT /GO within the fibers [40,43]. The nanofibers exhibited an entangled structure with a relatively uniform fiber distribution, contributing to a high surface area matrix. At higher magnification (Fig. 1b), smooth and continuous fiber strands were evident, with diameters in the nanometer to submicron range. The incorporation of MWCNT and GO within the PVA matrix was inferred from morphological variations and surface texture changes, though not visually isolated due to their nanoscale dispersion. The porous structure and high surface roughness of the electrospun mat are expected to enhance electron transfer and facilitate greater analyte interaction during electrochemical sensing [44]. Fig. 1c presents a higher magnification image, showing smooth fiber surfaces with consistent diameter throughout the field of view. The fibers appear well-separated, without signs of fusing or fiber flattening. Fig. 1d depicted the face wipe fabric morphology, where the diameter measurements of individual fibers showed a relatively narrow diameter distribution and the diameters obtained as 163.84 nm. Moreover, the presence of uniform pore spaces between the fibers may contribute to enhanced diffusion, breathability or active compound release in functional applications [45]. The images (Fig. 1c-d) further validate the homogeneity of fiber diameter and the absence of structural discontinuities. The interconnected fiber matrix suggests good mechanical integrity, while the surface smoothness and lack of agglomeration confirm effective dispersion of active agents (such as caffeine) within the matrix. The overall fabric condition appears stable and free from defects like fiber fusion or breakage, supporting the suitability of the fabric [46,47].

From Fig. 2a, the nanofibrous layer coated on the GCE electrode exhibited a semi-crystalline structure, as evidenced by a distinct diffraction peak observed at 2θ = 19.5º, which

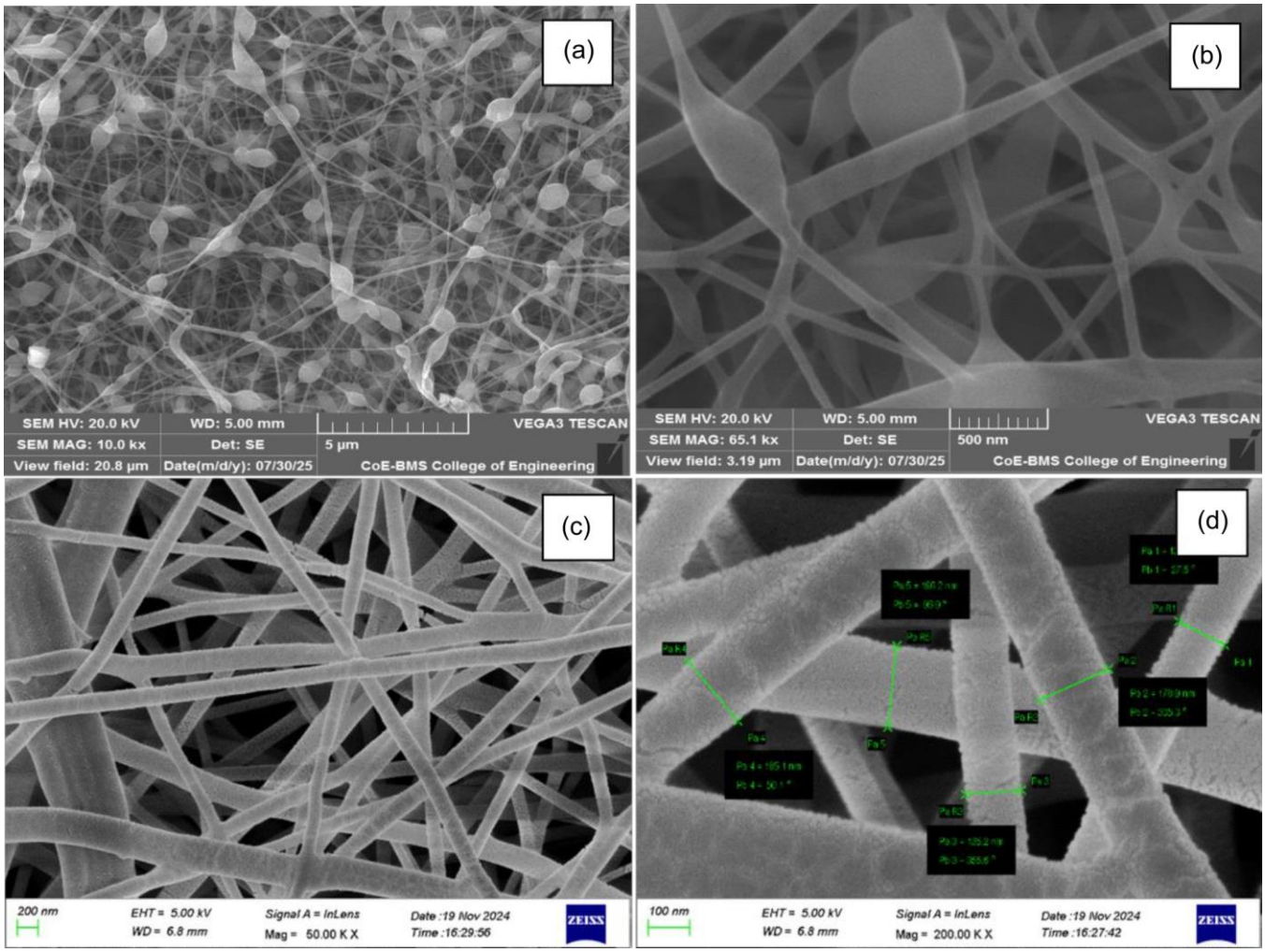

Fig. 1. SEM images of (a,b) the MGCE surface coated with the nanofiber, (c,d) Face wipe fabric surface under different scale bars

corresponds to PVA [48]. The incorporation of MWCNT and GO did not alter this peak, indicating that their addition did not influence the crystalline behaviour of the polymer. No additional diffraction peaks corresponding to MWCNT or GO were detected, suggesting their uniform distribution within the polymer matrix. The absence of characteristic peaks for both MWCNT and GO may be attributed to their effective dispersion across the nanofibers, as well as their low concentration in the composite formulation [49,50]. Also, the XRD pattern of face wipe fabric shown a broad diffraction peak at 19.58º. The broadening of the peaks is due to the amorphous nature of polyvinyl alcohol. An additional weak peak around 43º indicating the minor crystalline order of the polymer in it. The peaks correspond to the crystalline caffeine are 2θ = 14. 18º, 28.8º confirms the identity and purity of sample [50,51].

FTIR spectra: The FTIR spectra in Fig. 2b exhibited a strong broad band at ~ 3274 cm^{-1} attributed to O–H stretching vibration of the hydroxy group and at 2936 cm^{-1}, given asymmetric stretching vibration of CH_2 present in PVA. Also, the peaks at 1652 cm^{-1} correspond to the C=O carbonyl stretching and the peaks at 1417 and 1321.83 cm^{-1} corresponds to C–H bending vibration of CH_2 and C–H deformation vibration respectively. The peak at 1648 cm^{-1} indicating the carbonyl (C=O) stretching and the other peak 1088 cm^{-1} represents C–O stretching of acetyl groups and peak at 838 cm^{-1} indicate the presence of C-C stretching vibration [52-54]. In the spectrum of the face wipe fabric, characteristic caffeine peaks such as the C=O stretching band around 1700 cm^{-1} were not distinctly observed. In the spectrum, weak peaks were observed at 1581 cm^{-1} and 1238 cm^{-1} is attributed to the C=N/C=C stretching vibrations and C–N stretching vibrations of xanthine groups present in caffeine respectively [55,56]. Its appearance in the composite, despite the low caffeine content, also supports the incorporation of caffeine into the PVA matrix. Since, the caffeine was incorporated at a relatively small weight percentage compared to the PVA matrix, its vibrational signals may have been overlapped by dominant PVA bands. Moreover, at low loadings, weak signals from caffeine are often masked or merged within the broader polymer peaks. Despite the absence of clear caffeine peaks, the observed shift in the O–H stretching band from 3300 to 3274 cm^{-1} suggests intermolecular hydrogen bonding interactions, indicating the incorporation of caffeine into the polymer matrix.

Mechanical and solubility: Tensile testing was conducted and the material exhibited a peak force of 12.25 N corresponding to a tensile strength of 12.25 MPa as shown in Fig. 3. The elongation at peak load was measured as 1.949 mm, which corresponds to an overall elongation of 2.48%, indicating

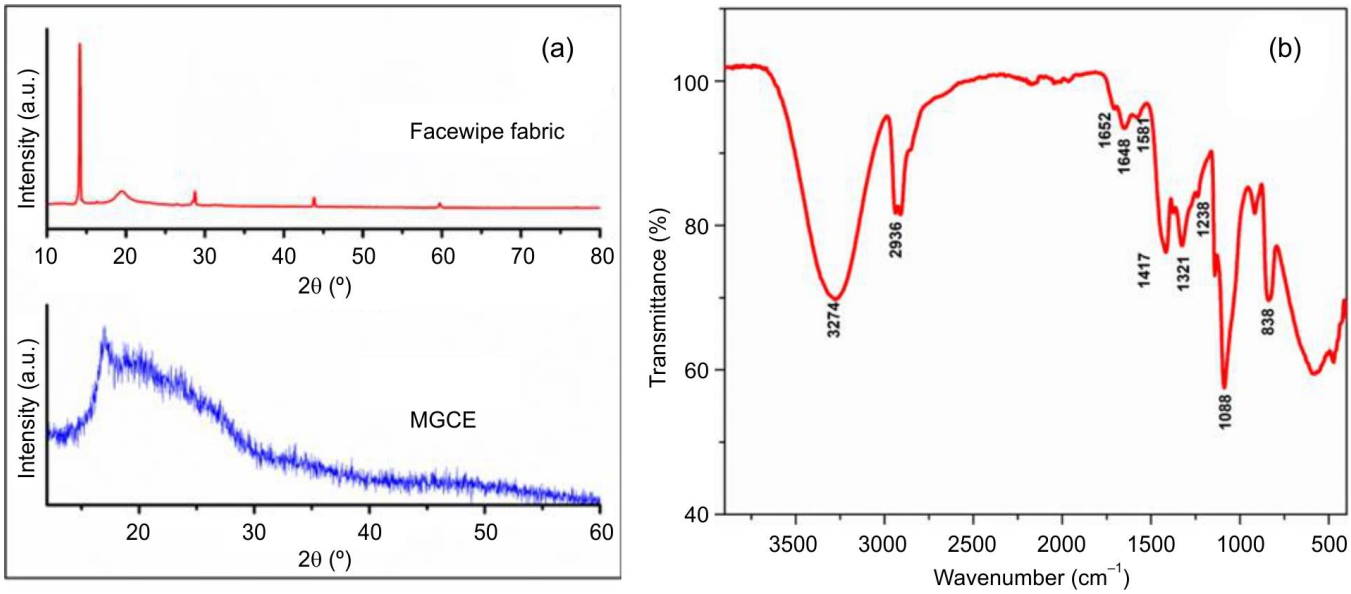

Fig. 2. (a) XRD spectra of MGCE surface coated nanofibers and face wipe fabric, (b) FTIR spectrum of face wipe fabric

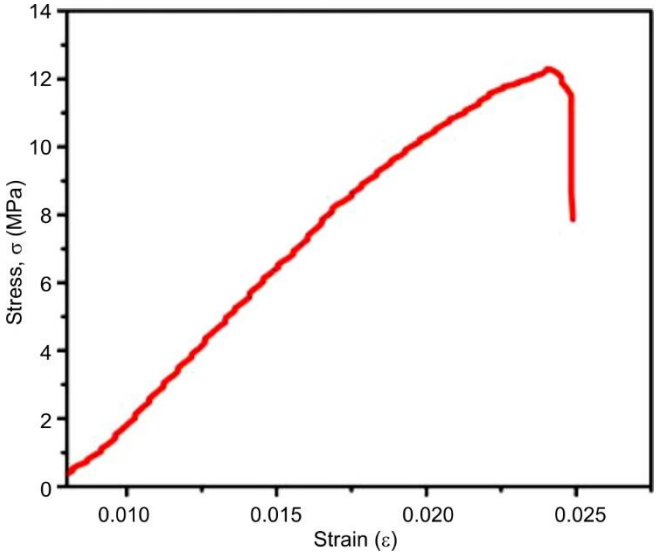

Fig. 3. Stress-strain curve of the electrospun face wipe fabric

limited ductility. From the linear region of the stress-strain curve, the Young's modulus was estimated to be 503 MPa, reflecting moderate stiffness. These results suggest that the fabricated nanofiber mat possesses sufficient tensile strength and rigidity, making it potentially suitable for applications requiring dimensional stability and mechanical durability [57,58].

The solubility of the PVA-caffeine composite matrix was determined to be 10.8%, indicating a high degree of structural stability in aqueous environments. This low solubility is a desirable characteristic for facial wipe applications, as it ensures that the wipe retains its mechanical integrity during storage and usage without premature disintegration. The limited solubility suggests that the PVA matrix maintains a stable polymeric network, preventing rapid dissolution upon contact with moisture. This property is crucial for prolonged shelf-life and user experience, as the wipe remains intact when wetted. The water absorption capacity of the wipe material was found to be 340%, demonstrating its exceptional moisture retention capability. This high degree of swelling is indicative of a highly porous and hydrophilic polymeric network, which is essential for efficient hydration delivery in skincare applications. The hydration ensures that the wipe remains sufficiently moist throughout application and the polymer matrix can act as a reservoir for caffeine, facilitating its gradual diffusion into the skin rather than an abrupt release. The interconnected porous structure of the material allows for rapid water penetration while maintaining structural coherence, ensuring uniform caffeine distribution [59-62].

Electrochemical behaviour: The calibration curves for caffeine detection using both bare GCE and MGCE electrodes across a concentration range of 0-5 mg/mL is shown in Fig. 4. The corresponding peak current responses show a strong linear relationship with increasing caffeine concentration in both electrodes. The linear equations and R^2 values obtained were: For bare GCE: I_p = 2.729x + 1.457, R^2 =

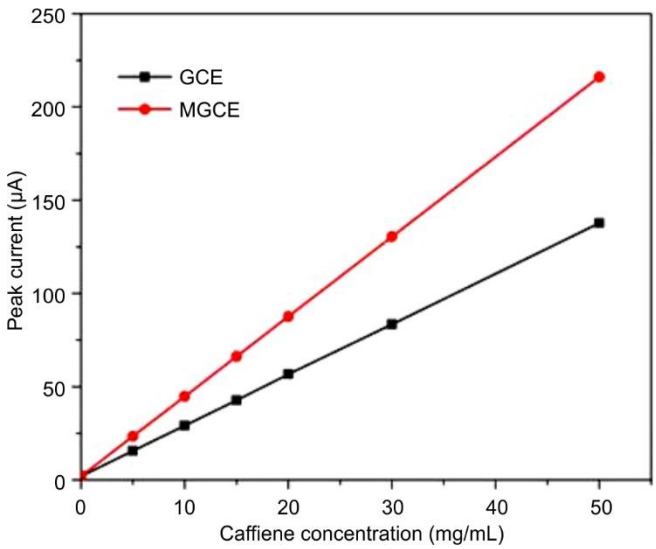

Fig. 4. Calibration plots for caffeine detection of bare GCE and MGCE

0.997; and for modified GCE: $I_p = 4.28x + 1.995$, $R^2 = 0.999$, where I_p is peak current and R is coefficient of determination. These results clearly indicate that the MGCE exhibits a higher slope, a greater current response per unit increase in caffeine concentration. The reason is attributed to the enhanced surface area and conductivity provided by the conductive particles present in the electrospun nanofibers, which facilitated better electron transfer kinetics and analyte interaction [63].

Fig. 5 presents a bar diagram comparing caffeine concentrations (mg) released at various time intervals (5-30 min) using GCE and MGCE electrodes. The data show a steady increase in caffeine release over time, indicating a controlled and sustained release from the face wipe matrix into water. This sustained release behaviour is particularly important for skincare applications, where prolonged exposure ensures effective absorption. The MGCE consistently yielded higher caffeine concentrations across all time points compared to the GCE. These results suggest that the modified electrode exhibits enhanced sensitivity and more efficient caffeine detection. The clearer observation of the caffeine release profile over time further confirms its superior capability in tracking gradual concentration changes.

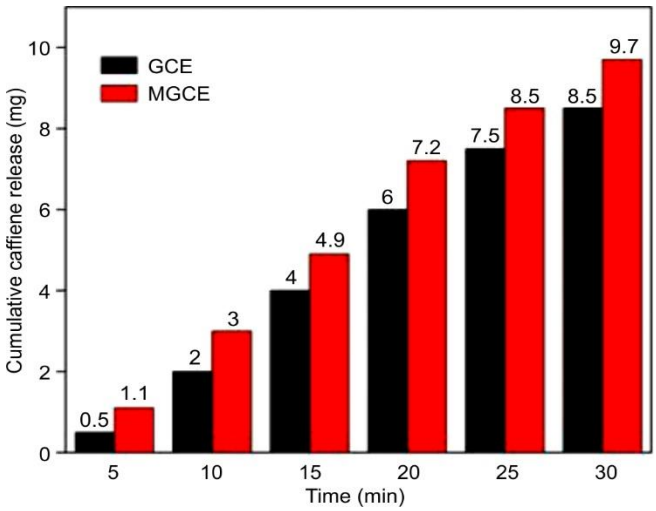

Fig. 5. Comparative bar chart showing the amount of caffeine (mg) at different time intervals using GCE and MGCE

The peak current values obtained from the LSV measurements of face wipe sample solutions recorded at different time intervals using both GCE and MGCE electrodes depicted in Fig. 6. The GCE detected a total caffeine release increasing from 1.593 μA at 5 min to 4.091 μA at 30 min. The MGCE, however, exhibited a more responsive behaviour, starting at 2.46 μA and reaching 6.14 μA at 30 min. These current increments directly correlate with increasing caffeine concentrations released into the medium, thus validating the slow-release characteristic of the face wipe over the 30 min period. The consistent rise in current (due to caffeine content) with time also proves that the face wipe is not releasing all the caffeine at once, but instead offering a time-dependent release profile, which is essential for formulations aimed at sustained skincare applications. From Fig. 5, it is clear that the maximum release was observed around the 30 min mark, identifying this time point as optimal for effective release from the wipe.

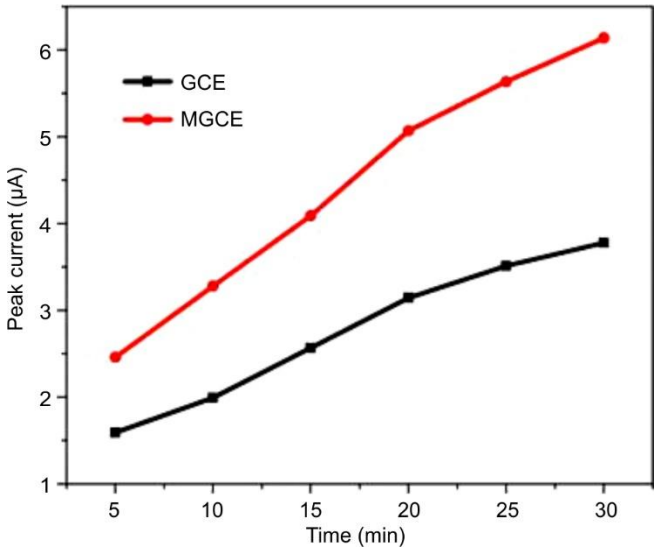

Fig. 6. Time-dependent caffeine release profile and peak current variation plots of GCE and MGCE

To assess the sensitivity and practical applicability of the electrochemical method for caffeine detection, the limit of detection (LOD) and limit of quantification (LOQ) were calculated for both the GCE and the MGCE. These parameters were determined using the standard deviation (σ) of blank measurements (n = 5) and the slope (S) of the calibration curves based on the following equations:

$$LOD = 3.3 \times (\sigma/S) \quad (3)$$

$$LOQ = 10 \times (\sigma/S) \quad (4)$$

For the GCE, the standard deviation of the blank sample was found to be 0.1233 μA and the slope of the calibration curve was 2.729. Accordingly, the LOD and LOQ were calculated as 0.1356 mg/mL and 0.452 mg/mL, respectively. This indicates that the bare electrode can reliably detect caffeine concentrations down to approximately 0.1356 mg/mL but can only be quantified accurately at or above 0.452 mg/mL. In contrast, the MGCE showed a significantly improved performance, with a lower standard deviation of 0.0594 μA and a higher calibration slope of 4.28. As a result, the LOD and LOQ values were 0.042 mg/mL and 0.139 mg/mL, respectively. These values confirm the enhanced sensitivity and reliability of the modified electrode in detecting even trace levels of caffeine. The lower LOD value observed in the MGCE is particularly advantageous in applications where low concentrations of analyte must be detected, such as in skin-contact products like face wipes. This enhanced sensitivity ensures that even small amounts of caffeine released during early time intervals (*e.g.* 5 min) can be effectively identified and monitored. The incorporation of MWCNT and GO in the electrospun PVA matrix significantly enhanced the electrochemical response of electrode, leading to a lower detection threshold and improved analytical performance [64].

The LSV comparison responses of 30 min caffeine release sample using both the GCE and MGCE electrodes is plotted as shown in Fig. 7. The aim is to analyse possible shift in the peak potential and the current response, indicating the efficiency of electron transfer on the electrode surfaces [65]. The GCE had a peak potential = 1.427 V, whereas the MGCE

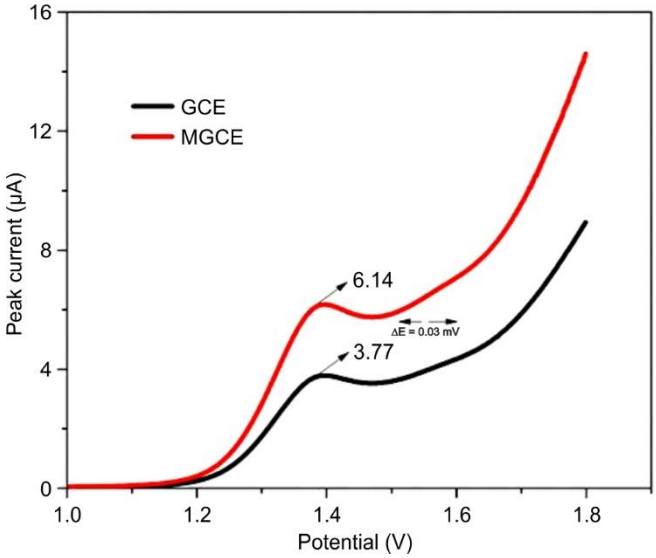

Fig. 7. LSV profiles of caffeine release recorded using plots of GCE and MGCE (comparison of peak potential shift)

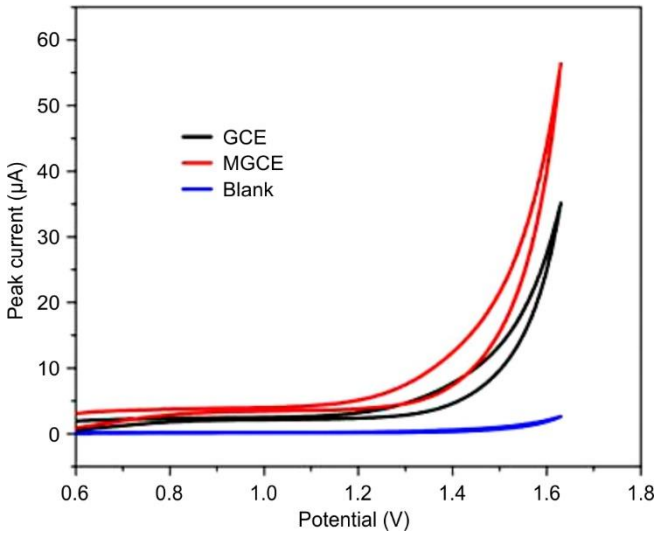

Fig. 8. Cyclic voltammetry comparison of 0.1 M KCl blank, GCE and MGCE with caffeine release sample at 30 min, recorded at a scan rate of 50 mV/s

possessed peak potential value of 1.397 V, where the shift in peak potential to a less positive value (ΔE = -0.03 V) with the modified electrode suggests faster electron transfer kinetics and improved conductivity due to the MWCNT and GO nanofiber modification. Furthermore, the MGCE showed a significantly higher peak current, highlighting its enhanced electrocatalytic activity and sensitivity for caffeine detection. The modification facilitates easier oxidation of caffeine molecules, reducing the required energy for the electrochemical reaction.

Cyclic voltammetry (CV): To evaluate the electrochemical performance and sensing efficiency of the modified electrode toward caffeine release, the CV was performed at a fixed scan rate of 50 mV/s using blank (0.1 M KCl), GCE and the MGCE, respectively. As shown in the CV plot (Fig. 8), the peak current response for blank electrolyte (0.1 M KCl without caffeine) was minimal (~2.82 μA), indicating negligible Faradaic activity and confirming the electrochemical stability of the background medium. Upon introduction of the caffeine-loaded sample, a significant increase in the oxidation peak current was observed for both the bare and modified GCEs. The GCE exhibited a peak current of ~35 μA, demonstrating its capability to detect caffeine release. However, the MGCE exhibited a remarkably higher peak current of ~56 μA under identical conditions, indicating enhanced electrochemical sensitivity and improved charge transfer kinetics. This enhancement can be attributed to the higher surface area, increased adsorption capacity and improved electron transport pathways provided by the electrospun nanofiber matrix functionalized with conductive and active components. The substantial increase in peak current observed for the MGCE, compared to the GCE and blank, clearly establishes the superior electrochemical sensing performance of the modified electrode for caffeine detection [66].

To monitor the time-dependent release behaviour of caffeine from the impregnated face wipe, CV was performed at a fixed scan rate of 50 mV/s for samples collected at 5, 10, 15, 20, 25 and 30 min. The study was conducted using both GCE and the MGCE. As shown in Fig. 9, a gradual increase

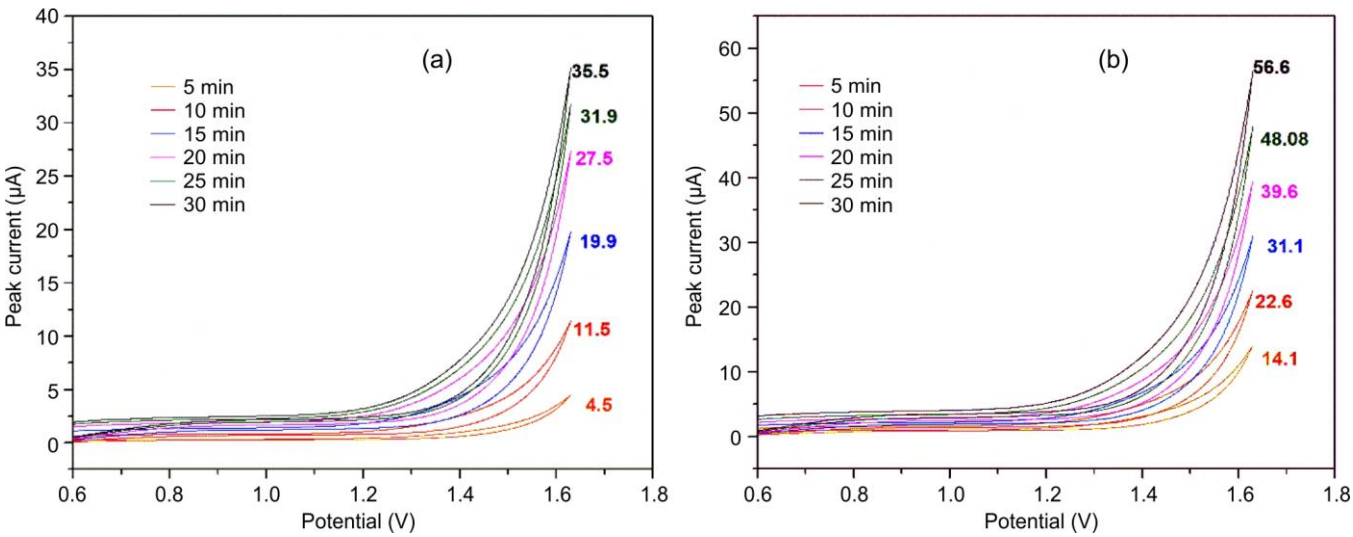

Fig. 9. Cyclic voltammetry plots showing time-dependent release profiles of caffeine (5-30 min) recorded at 50 mV/s using (a) GCE and (b) MGCE

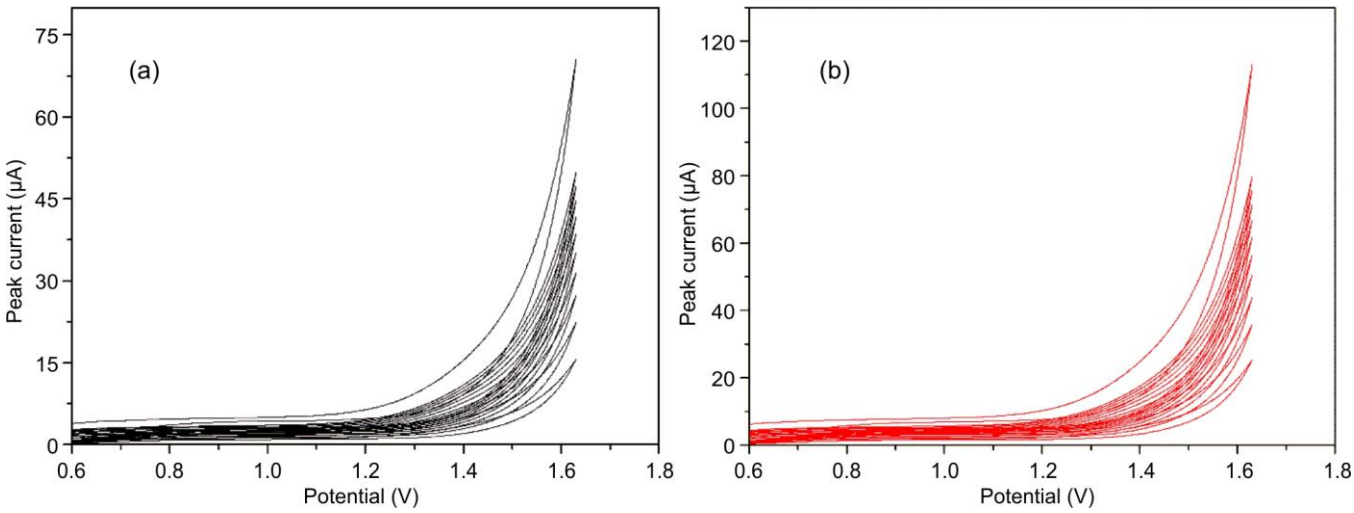

Fig. 10. Cyclic voltammetry of (a) GCE and (b) MGCE at varying scan rates

in peak current was observed with increasing release time for both electrodes. This trend confirms the sustained release of caffeine into the medium over time. The increase in electrochemical response corresponds to the higher concentration of caffeine diffused from the wipe into the electrolyte. This comparative time-dependent analysis also demonstrates that the modified electrode (b) is more efficient in tracking release kinetics, making it a superior candidate for controlled-release monitoring applications.

Comparing the cyclic voltammograms recorded in Fig. 10, the MGCE exhibited a significantly higher current response than the GCE at all scan rates. This clearly demonstrates the enhancement in electrochemical performance due to the electrode modification with PVA, MWCNT and GO nanofibers. As with the GCE, the increase in peak current with scan rate indicates a redox process that is influenced by the scan rate. To confirm the mechanism, linear plots were constructed for both the square root of scan rate (Fig. 11) and the logarithmic relationship (Fig. 12).

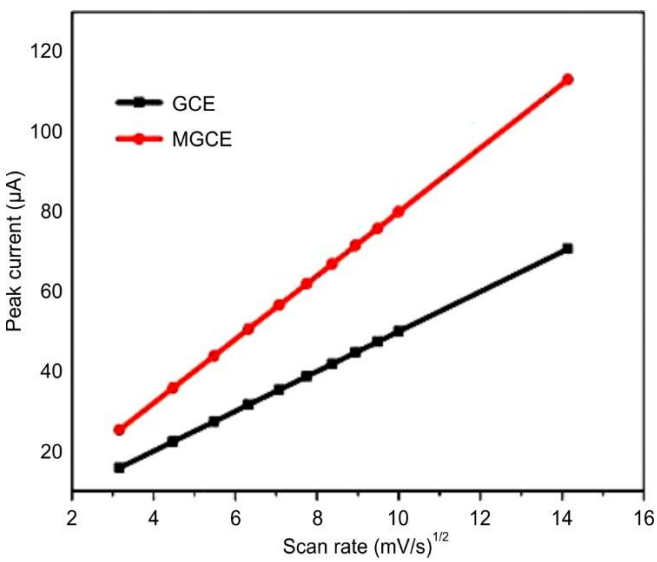

Fig. 11. Linear plot of peak current *vs.* square root of scan rate plots of GCE and MGCE

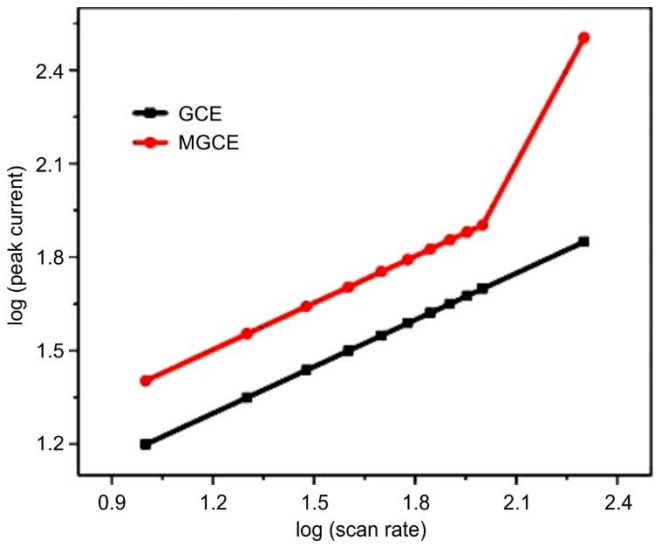

Fig. 12. Log-Log plot of scan rate *vs.* peak current plots of GCE and MGCE

From Fig. 9, obtained the linear relationship between the peak current (I_p) and the square root of the scan rate ($v^{1/2}$) for both bare and modified electrodes. For GCE: Slope = 4.999, R^2 = 0.998; For modified GCE: Slope = 8.004, R^2 = 0.999. Both electrodes exhibited excellent linearity (R^2 > 0.99), confirming that the oxidation of caffeine follows a diffusion-controlled electrochemical process at both surfaces. However, the steeper slope for the MGCE suggests enhanced electron transfer and improved analyte diffusion at the electrode interface, likely due to the increased surface area and conductivity provided by the MWCNT-GO-PVA nanofiber modification. It further reinforces that the electrode modification not only increased sensitivity but also preserved the diffusion-based nature of the redox process.

The double logarithmic plots of peak current (log I_p) *versus* scan rate (log v) for both bare and modified electrodes represented in Fig. 12. This analysis further confirms the kinetics of the electrochemical process.

The obtained linear regression equations and corresponding parameters are:

For GCE:

$$\log I_p = 0.4973 \times \log \nu + 0.699, R^2 = 0.9997; \text{ and}$$

For MGCE:

$$\log I_p = 0.7046 \times \log \nu + 0.5933, R^2 = 0.911$$

In case of the GCE, the slope of 0.4973 confirms a purely diffusion-controlled mechanism and for the MGCE, the slope increases to 0.7046, suggesting a mixed control mechanism, where both diffusion and adsorption may contribute to the electron transfer kinetics. This is attributed to the enhanced surface interaction between caffeine molecules and the modified electrode's nanostructured surface, which facilitates the partial adsorption behaviour. Thus, while both electrodes demonstrate diffusion dominance, the MGCE introduces additional interactions that improve the overall sensitivity and allow better control over analyte binding and release made it particularly suitable for time-dependent release monitored in the caffeine face wipe fabric.

Conclusion

In this study, a PVA based electrospun face wipe fabric infused with caffeine was prepared and characterized. The face wipe was systematically evaluated for its time-dependent caffeine release profile and electrochemical sensing performance. The LSV was employed to quantify the amount of caffeine released at regular intervals using both bare and modified electrodes. The MGCE exhibited significantly enhanced sensitivity, with a higher peak current and improved LOD/LOQ values, demonstrating its superior analytical performance. The CV studies conducted at various scan rates revealed insights into the electrode kinetics. The GCE showed a linear relationship between peak current and the square root of scan rate, confirming a diffusion-controlled mechanism. In contrast, the MGCE followed a mixed diffusion-adsorption behaviour, as evident from its higher slope value and peak current response. The morphology of the nanofibrous wipe, confirmed through SEM analysis, showed uniform, bead-free fibers with good porosity and structural integrity, supporting effective caffeine encapsulation and release. The fabricated face wipe fabric represents a promising, cost-effective platform for real-time monitoring of active compounds in personal care applications.

CONFLICT OF INTEREST

The authors declare that there is no conflict of interests regarding the publication of this article.

REFERENCES

1. B.A. Reta, K.M. Babu and T. Tesfaye, *AATCC J. Res.*, **11**, 73 (2024); https://doi.org/10.1177/2472344423121544
2. R. Guru and A.K. Choudhary, *Asian Text. J.*, **28**, 49 (2019).
3. H.G. Atasağun and G.S. Bhat, *J. Ind. Text.*, **49**, 722 (2020); https://doi.org/10.1177/1528083718795910
4. J.M. Boyce, *Am. J. Infect. Control*, **49**, 104 (2021); https://doi.org/10.1016/j.ajic.2020.06.183
5. K.J. Rodriguez, C. Cunningham, R. Foxenberg, D. Hoffman and R. Vongsa, *Pediatr. Dermatol.*, **37**, 447 (2020); https://doi.org/10.1111/pde.14112
6. S. Durukan and F. Karadagli, *Sci. Total Environ.*, **697**, 134135 (2019); https://doi.org/10.1016/j.scitotenv.2019.134135
7. T. Hadley, K. Hickey, K. Lix, S. Sharma, T. Berretta and T. Navessin, *BioResources*, **18**, 2271 (2023); https://doi.org/10.15376/biores.18.1.Hadley
8. G. Fytianos, A. Rahdar and G.Z. Kyzas, *Nanomaterials*, **10**, 979 (2020); https://doi.org/10.3390/nano10050979
9. A.A. Keller and C.A. Arturo Keller, *Int. J. Cosmet. Sci.*, **45(S1)**, 127 (2023); https://doi.org/10.1111/ics.12905
10. S.H. Tekinay, *Eur. Polym. J.*, **217**, 113311 (2024); https://doi.org/10.1016/j.eurpolymj.2024.113311
11. M. Pereira-Silva, A.M. Martins, I. Sousa-Oliveira, H.M. Ribeiro, F. Veiga, J. Marto and A.C. Paiva-Santos, *Acta Biomater.*, **142**, 14 (2022); https://doi.org/10.1016/j.actbio.2022.02.025
12. V. Palmieri, F. De Maio, M. De Spirito and M. Papi, *Nano Today*, **37**, 101077 (2021); https://doi.org/10.1016/j.nantod.2021.101077
13. L. Xiong, H. He, J. Tang, Q. Yang and L. Li, Oxid. Med. Cell. Longev., **2022**, 2422618 (2022); https://doi.org/10.1155/2022/2422618
14. J. Teno, M. Pardo-Figuerez, N. Hummel, V. Bonin, A. Fusco, C. Ricci, G. Donnarumma, M.B. Coltelli, S. Danti and J.M. Lagaron, *Cosmetics*, **7**, 96 (2020); https://doi.org/10.3390/cosmetics7040096
15. P. Tipduangta, W. Watcharathirawongs, P. Waritdecha, B. Sirithunyalug, P. Leelapornpisid, W. Chaiyana and C.F. Goh, *J. Drug Deliv. Sci. Technol.*, **86**, 104732 (2023); https://doi.org/10.1016/j.jddst.2023.104732
16. N. Asthana, K. Pal, A.A.A. Aljabali, M.M. Tambuwala, F.G. de Souza and K. Pandey, *J. Mol. Struct.*, **1229**, 129592 (2021); https://doi.org/10.1016/j.molstruc.2020.129592
17. T. Wasilewski and T. Bujak, *Ind. Eng. Chem. Res.*, **53**, 13356 (2014); https://doi.org/10.1021/ie502163d
18. O.J. Yoon, *Porrime*, **40**, 985 (2016); https://doi.org/10.7317/pk.2016.40.6.985
19. Y. Zhang, C. Zhang and Y. Wang, *Nanoscale Adv.*, **3**, 6040 (2021); https://doi.org/10.1039/D1NA00508A
20. I. Aranaz, N. Acosta, C. Civera, B. Elorza, J. Mingo, C. Castro, M. Gandía and A. Heras Caballero, *Polymers*, **10**, 213 (2018); https://doi.org/10.3390/polym10020213
21. L.K. Al-Halaseh, S.K. Tarawneh, N.A. Al-Jawabri, W.K. Al-Qdah, M.N. Abu-Hajleh, A.M. Al-Samydai and M.A. Ahmed, *J. Appl. Pharm. Sci.*, **12**, 34 (2022); https://doi.org/10.7324/JAPS.2022.120703
22. Y. Jia, C. Yang, X. Chen, W. Xue, H.J. Hutchins-Crawford, Q. Yu, P.D. Topham and L. Wang, *J. Mater. Chem. C Mater. Opt. Electron. Devices*, **9**, 9042 (2021); https://doi.org/10.1039/D1TC01477C
23. Y. Hong, K. Fujimoto, R. Hashizume, J. Guan, J.J. Stankus, K. Tobita and W.R. Wagner, *Biomacromolecules*, **9**, 1200 (2008); https://doi.org/10.1021/bm701201w
24. Z. Zhang, H. Liu, D.G. Yu and S.W.A. Bligh, *Biomolecules*, **14**, 789 (2024); https://doi.org/10.3390/biom14070789
25. A. Hernández-Rangel and E.S. Martin-Martinez, *J. Biomed. Mater. Res. A*, **109**, 1751 (2021); https://doi.org/10.1002/jbm.a.37154.
26. K. Huang, Y. Si, C. Guo and J. Hu, *Adv. Colloid Interface Sci.*, **331**, 103236 (2024); https://doi.org/10.1016/j.cis.2024.103236

27. H. Jiang, L. Wang and K. Zhu, *J. Control. Release*, **193**, 296 (2014); https://doi.org/10.1016/j.jconrel.2014.04.025
28. N. Laosirisathian, C. Saenjum, J. Sirithunyalug, S. Eitssayeam, W. Chaiyana and B. Sirithunyalug, *Fibers Polym.*, **22**, 36 (2021); https://doi.org/10.1007/s12221-021-0165-0
29. F. Rostami, J. Yekrang, N. Gholamshahbazi, M. Ramyar and P. Dehghanniri, *Emergent Mater.*, **6**, 1903 (2023); https://doi.org/10.1007/s42247-023-00587-9
30. K. Ramya and K. Amrutha, International Conference on Advances in Technical Textiles, Bannari Amman Institute of Technology, Sathyamangalam, India p. 61 (2021).
31. J.M. Chin, M.L. Merves, B.A. Goldberger, A. Sampson-Cone and E.J. Cone, *J. Anal. Toxicol.*, **32**, 702 (2008); https://doi.org/10.1093/jat/32.8.702
32. H.N. Wanyika, E. Gatebe, L. Gitu and E. Ngumba, *Afr. J. Food Sci.*, **4**, 353 (2010).
33. T. Koláčková, K. Kolofiková, I. Sytařová, L. Snopek, D. Sumczynski and J. Orsavová, *Plant Foods Hum. Nutr.*, **75**, 48 (2020); https://doi.org/10.1007/s11130-019-00777-z
34. M.J. Visconti, W. Haidari and S.R. Feldman, *J. Dermatol. Dermatol. Surg.*, **24**, 18 (2020); https://doi.org/10.4103/jdds.jdds_52_19
35. T. Natasha, L. Wijaya, T. Djuartina and Z. Arieselia, *J. Urban Heal. Res.*, **3**, 1 (2024); https://doi.org/10.25170/juhr.v3i1.5467
36. S.W. Koo, S. Hirakawa, S. Fujii, M. Kawasumi and P. Nghiem, *Br. J. Dermatol.*, **156**, 957 (2007); https://doi.org/10.1111/j.1365-2133.2007.07812.x
37. Y.P. Tseng, C. Liu, L.P. Chan and C.H. Liang, *J. Cosmet. Dermatol.*, **21**, 2189 (2022); https://doi.org/10.1111/jocd.14341
38. R. Liao, T. Parker, K. Bellerose, D. Vollmer and X. Han, *Cosmetics*, **9**, 96 (2022); https://doi.org/10.3390/cosmetics9050096
39. C. Blanco-Llamero, H.F. Macário, B.N. Guedes, F. Fathi, M.B.P.P. Oliveira and E.B. Souto, *Cosmetics*, **11**, 149 (2024); https://doi.org/10.3390/cosmetics11050149
40. H. Du, X. Chen, H. Ding, X. Yin, Y. Su and G.J. Weng, *Compo. Commun.*, **53**, 102196 (2025); https://doi.org/10.1016/j.coco.2024.102196
41. V. Rubentheren, T.A. Ward, C.Y. Chee and C.K. Tang, *Carbohydr. Polym.*, **115**, 379 (2015); https://doi.org/10.1016/j.carbpol.2014.09.007
42. S. Rahman, A. Konwar, G. Majumdar and D. Chowdhury, *Carbohydr. Polym.*, **2**, 100158 (2021); https://doi.org/10.1016/j.carpta.2021.100158
43. X. Wu, F. Mu and H. Zhao, *J. Mater. Sci. Technol.*, **55**, 16 (2020); https://doi.org/10.1016/j.jmst.2019.05.063
44. P. Wang, H. Lv, X. Cao, Y. Liu and D.G. Yu, *Polymers*, **15**, 921 (2023); https://doi.org/10.3390/polym15040921
45. F. Zhang, Y. Si, J. Yu and B. Ding, *Chem. Eng. J.*, **456**, 140989 (2023); https://doi.org/10.1016/j.cej.2022.140989
46. G.C. Türkoğlu, N. Khomarloo, E. Mohsenzadeh, D.N. Gospodinova, M. Neznakomova and F. Salaün, *Int. J. Mol. Sci.*, **25**, 1668 (2024); https://doi.org/10.3390/ijms25031668
47. N. Soni, D. Roy, D.M. Patel, P. Dhandhukia and J.N. Thakker, *Discover Chem.*, **2**, 57 (2025); https://doi.org/10.1007/s44371-025-00132-z
48. M. Tavassoli, B. Bahramian, R. Abedi-Firoozjah, N. Jafari, H. Javdani, S.M. Sadeghi, S. Hadavifar, S. Majnouni, A. Ehsani and S. Roy, *Food Bioprocess Technol.*, **18**, 3223 (2025); https://doi.org/10.1007/s11947-024-03637-0
49. M.I. Mohammed, H.Y. Zahran, S. Zyoud, I.S. Yahia and A.M. Ismail, *J. Mater. Sci. Mater. Electron.*, **35**, 515 (2024); https://doi.org/10.1007/s10854-024-12144-z
50. E. Schnitzler, M. Kobelnik, G.F.C. Sotelo, G. Bannach and M. Ionashiro, *Eclét. Quím.*, **29**, 71 (2004); https://doi.org/10.26850/1678-4618eqj.v29.1.2004.p71-78
51. X. Li, M.A. Kanjwal, L. Lin and I.S. Chronakis, *Colloids Surf. B Biointerfaces*, **103**, 182 (2013); https://doi.org/10.1016/j.colsurfb.2012.10.016
52. A. Kharazmi, N. Faraji, R. Mat Hussin, E. Saion, W.M.M. Yunus and K. Behzad, *Beilstein J. Nanotechnol.*, **6**, 529 (2015); https://doi.org/10.3762/bjnano.6.55
53. H.S. Mansur, C.M. Sadahira, A.N. Souza and A.A.P. Mansur, *Mater. Sci. Eng. C*, **28**, 539 (2008); https://doi.org/10.1016/j.msec.2007.10.088
54. M.A. Abureesh, A.A. Oladipo and M. Gazi, *Int. J. Biol. Macromol.*, **90**, 75 (2016); https://doi.org/10.1016/j.ijbiomac.2015.10.001
55. S. Butt, S.M.F. Hasan, M.M. Hassan, K.M. Alkharfy and S.H. Neau, *Saudi Pharm. J.*, **27**, 619 (2019); https://doi.org/10.1016/j.jsps.2019.03.002
56. Y. Daghbouche, S. Garrigues, M.T. Vidal and M. de la Guardia, *Anal. Chem.*, **69**, 1086 (1997); https://doi.org/10.1021/ac960693v
57. M. Koosha and H. Mirzadeh, *J. Biomed. Mater. Res. A*, **103**, 3081 (2015); https://doi.org/10.1002/jbm.a.35443
58. N.A.M. Salleh, A.M. Afifi, F.M. Zuki and H.S. SalehHudin, *Beilstein J. Nanotechnol.*, **16**, 286 (2025); https://doi.org/10.3762/bjnano.16.22
59. D. Nataraj, R. Reddy and N. Reddy, *Eur. Polym. J.*, **124**, 109484 (2020); https://doi.org/10.1016/j.eurpolymj.2020.109484
60. J.C. Park, T. Ito, K.O. Kim, K.W. Kim, B.S. Kim, M.S. Khil, H.Y. Kim and I.S. Kim, *Polym. J.*, **42**, 273 (2010); https://doi.org/10.1038/pj.2009.340
61. T.H.N. Vu, S.N. Morozkina, R.O. Olekhnovich, A.V. Podshivalov and M.V. Uspenskaya, *Polymers*, **16**, 3393 (2024); https://doi.org/10.3390/polym16233393
62. Z. Guo, Y. Bi, Z. Wu and C. Yuan, *Wear*, **571**, 205786 (2025); https://doi.org/10.1016/j.wear.2025.205786
63. E. Murugan, A. Poongan, M. Kesava and A. Vinitha, *Indian J. Chem. Technol.*, **29**, 713 (2022).
64. A. Carolina Torres, M.M. Barsan and C.M.A. Brett, *Food Chem.*, **149**, 215 (2014); https://doi.org/10.1016/j.foodchem.2013.10.114
65. L. Švorc, *Int. J. Electrochem. Sci.*, **8**, 5755 (2013); https://doi.org/10.1016/S1452-3981(23)14720-1
66. A. Nasriddinov, S. Tokarev, V. Platonov, A. Botezzatu, O. Fedorova, M. Rumyantseva and Y. Fedorov, *Molecules*, **27**, 5058 (2022); https://doi.org/10.3390/molecules27165058